Identifying long-range structure in the intrinsically unstructured transactivation domain of p53

ARTICLE *in* PROTEINS STRUCTURE FUNCTION AND BIOINFORMATICS · MAY 2007

Impact Factor: 2.63 · DOI: 10.1002/prot.21364 · Source: PubMed

5 AUTHORS, INCLUDING:

Gary W Daughdrill
University of South Florida

45 PUBLICATIONS **1,262** CITATIONS

SEE PROFILE

PROTEINS: Structure, Function, and Bioinformatics 67:526–530 (2007)

SHORT COMMUNICATION

Identifying Long-Range Structure in the Intrinsically Unstructured Transactivation Domain of p53

Pamela Vise, Bharat Baral, Amber Stancik, David F. Lowry, and Gary W. Daughdrill*
Department of Microbiology, Molecular Biology, and Biochemistry, University of Idaho, Moscow, Idaho 83844-3052

ABSTRACT **Paramagnetic relaxation enhancement (PRE) was used to identify a compact dynamic structure for the intrinsically unstructured transactivation domain of the tumor suppressor protein, p53. Our results show that p53 residues essential for binding to the ubiquitin ligase, MDM2, and the 70 kDa subunit of replication protein A, RPA70, are separated by an average distance of 10–15 Å. This result suggests that a more extended member of the ensemble must be populated prior to binding either MDM2 or RPA70. We also show that PRE can be used to detect intermolecular distances between p53 and RPA70. Proteins 2007;67:526–530.** © 2007 Wiley-Liss, Inc.

Key words: ensemble; distance; paramagnetic; relaxation; enhancement

INTRODUCTION

The ability of intrinsically unstructured proteins (IUPs) to participate in complex regulatory processes is the basis for an expanding model of protein structure and function.[1–6] In this expanding model, IUPs form dynamic structures that are rapidly interconverting between multiple conformations and their biological function depends on this dynamic structure in the same way as the biological function of compact globular proteins depends on a relatively rigid structure.

IUPs are prevalent in eukaryotic signaling networks because they can remodel their structure to interact with multiple binding partners.[2,5,7] Eukaryotic transactivation domains (TADs) are intrinsically unstructured and their ability to interact with target proteins is mediated by the thermodynamic coupling of protein folding and binding.[1,2,8–10] Residues 1–73 of the tumor suppressor protein, p53, form a TAD (p53TAD) that is responsible for regulating p53 activity.[11] This domain contains binding sites for the ubiquitin ligase, MDM2, and the 70 kDa subunit of replication protein A, RPA70. When bound to MDM2, p53 becomes ubiquinated and targeted for degradation. When bound to RPA70, p53 may be stabilized and available to amplify the cellular response to DNA damage.[9] It is unclear if the binding of p53 to MDM2 and RPA70 is mutually exclusive.

There is a paucity of atomic models for IUPs and determining high resolution atomic structures for IUPs, like p53TAD, is difficult because they are resistant to crystallization and traditional methods for measuring internuclear distances using NMR. The lack of atomic structures for IUPs significantly limits our understanding of the relationship between their dynamic structure and biological function. To overcome this limitation, new approaches and methodology must be developed that permit the identification of long-range distances in an ensemble of rapidly interconverting structures.

Paramagnetic relaxation enhancement (PRE) is an important technique for determining the atomic structures of IUPs because it can be used to identify average distances between 10 and 30 Å in a dynamic structure.[12–14] PRE depends on the magnetic interaction between an unpaired electron and a proton. This interaction increases the transverse relaxation rate of the proton by a factor that is proportional to the $1/\langle r^6 \rangle$ distance from the electron.

In this report, PRE was used to measure average intramolecular distances for p53TAD. The presence of long range distances in p53TAD provides evidence for a compact dynamic structure. In particular, we show that the binding sites for MDM2 and RPA70 are separated by an average distance of 10–15 Å. Identifying the average intramolecular distances for IUPs is a necessary step in determining their population-weighted ensemble-average structures. Knowledge of these structures can ultimately be used to predict function. We also show that PRE can be applied to the problem of measuring intermolecular distances between IUPs and their binding partners.

Grant sponsor: ACS; Grant number: IRG7700323; Grant sponsor: NIH; Grant number: P20 RR 16448.

*Correspondence to: Gary W. Daughdrill, Department of Microbiology, Molecular Biology, and Biochemistry, University of Idaho, Life Science South Rm. 140, Moscow, ID 83844-3052.
E-mail: gdaugh@uidaho.edu

Received 2 October 2006; Revised 23 October 2006; Accepted 12 December 2006

Published online 2 March 2007 in Wiley InterScience (www.interscience.wiley.com). DOI: 10.1002/prot.21364

MATERIALS AND METHODS

Protein Purification and NMR Data Collection

Development of the expression plasmid for p53TAD was previously described.[9] This plasmid was used as a template for constructing single cysteine mutants at positions E28 and D61 using the Stratagene quikchange mutagenesis protocol. Purification of unlabeled and ^{15}N-labeled D61C and ^{15}N-labeled and ^{15}N- ^{13}C-labeled E28C was also based on previously described methods.[9] Finally, all NMR experiments were performed as previously described using a Varian Inova spectrometer operating at a ^{1}H resonance frequency of 600 MHz and a sample temperature of 298 K.[9]

Backbone Resonance Assignments of Cysteine Mutants

The backbone resonance assignments of wild type p53TAD were reported previously.[9] Small chemical shift changes were observed for the resonances in the ^{15}N HSQC spectrum of D61C when compared with wild type p53TAD. The amide nitrogen and proton resonance assignments for D61C were made by assuming a minimal perturbation in ^{15}N HSQC spectrum. The amide nitrogen and proton resonance assignments for E28C were made using the standard triple resonance methods that were applied to wild type p53TAD.[9] Analysis of C_α and C_β chemical shifts were used to determine that the changes observed in the ^{15}N HSQC spectrum of E28C were not accompanied by structural changes.

MTSL Labeling and NMR Data Analysis

To induce PRE, the spin label MTSL is covalently attached to the free thiol of the cysteine residues in the p53TAD mutants. The cysteines are maintained in their reduced forms using a buffer containing dithiothreitol (DTT). The DTT is rapidly exchanged using a gravity flow desalting column (PD10) and the MTSL is added directly to the protein fractions and incubated at room temperature for 1 h. Excess MTSL is removed using another PD10 column and the MTSL labeled protein is concentrated for NMR analysis. For all of the samples, the extent of the MTSL labeling is verified to be greater than 95% using mass spectrometry.

Three ^{15}N HSQC spectra are collected on each cysteine mutant. One spectrum is collected on the MTSL labeled mutant, one spectrum is collected on the MTSL labeled mutant after the spin label is reduced with ascorbic acid, and one spectrum is collected on a concentration matched sample of the cysteine mutant without the spin label. The resonance intensity quotient is determined by measuring the peak intensities from all three experiments and dividing the MTSL intensities by the reduced and unlabeled resonance intensities. Comparison of the resonance intensity quotients from the labeled and unlabeled cystene mutants verified that a sufficient amount of ascorbic acid was added to reduce the spin label. Both resonance intensity quotients were identical to within 5%.

Calculation of Distances

To convert the PRE data into distances, the integrated intensities of resolved HSQC resonances were measured. The resonance intensity quotient for a particular residue was calculated as I_{ox}/I_{red}, where I_{ox} is the resonance intensity in the oxidized state, I_{red} is the resonance intensity of either the MTSL labeled protein following the addition of ascorbic acid or the unlabeled protein. ^{15}N spin relaxation, longitudinal ^{1}H relaxation, and the difference between in-phase and anti-phase transverse ^{1}H magnetization were ignored because these effects contribute only small corrections to the calculated electron–proton target distances. These approximations, together with a measurement of the intrinsic proton transverse relaxation rate in the reduced state, allow a fit of the contribution of the spin label to the proton transverse relaxation rate.[15] In our study, the intrinsic proton transverse relaxation rate was measured by fitting the HSQC resonances to a Lorentzian function and calculating the average value. In the HSQC experiments, the proton was transverse during the INEPT delays for a total of 9.8 ms.

Once the paramagnetic contribution to proton transverse relaxation is determined, the electron–proton distance is calculated using standard relaxation theory, assuming the electron–proton correlation time is similar to the average overall rotational correlation time of the proton-nitrogen vectors obtained from reduced spectral density mapping of the ^{15}N relaxation data for the WT protein.[9] The overall correlation time for individual residues varied from 3 to 5 ns. However, the calculation of proton–electron distances is insensitive to changes in correlation time of 50%.[13] In our analysis, the average rotational correlation time from model-free analysis was measured and found to be 3.3 ns.

RESULTS AND DISCUSSION

Intramolecular PRE for p53TAD

To measure intramolecular PRE for p53TAD, a ^{15}N-labeled mutant that replaced the glutamic acid at position 28 with a cysteine (E28C) was purified and the nitrosyl spin label, MTSL, was covalently attached to the free thiol of C28. MTSL contains an unpaired electron that will induce PRE in nearby protons. The distance from the spin label to the backbone amide protons can be estimated based on the ^{15}N HSQC resonance intensity quotient for the oxidized and reduced forms of the MTSL labeled protein. Figure 1 shows the resonance intensity quotient for E28C plotted as a function of residue number. The position of the MTSL is shown with the arrow. To obtain the resonance intensity quotients shown in Figure 1, ^{15}N HSQC spectra were collected for MTSL labeled E28C before and after the addition of a fivefold molar excess of ascorbic acid.

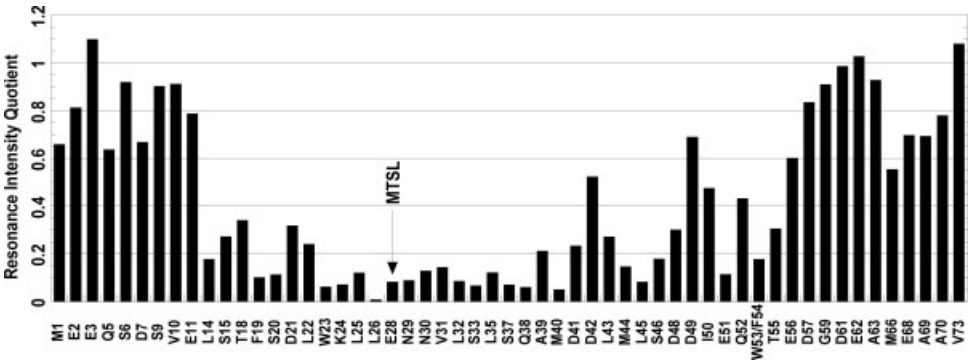

Fig. 1. Intramolecular PRE for E28C. The vertical axis shows the E28C resonance intensity quotient and the horizontal axis shows the p53TAD residues. Resonance intensity measurements were made on a ^{15}N-labeled sample of E28C following attachment of MTSL to C28. The MTSL label was reduced by adding a fivefold molar excess of ascorbic acid and the resonance intensity measurements were repeated. The extent of MTSL labeling for E28C was verified to be >95% using mass spectrometry.

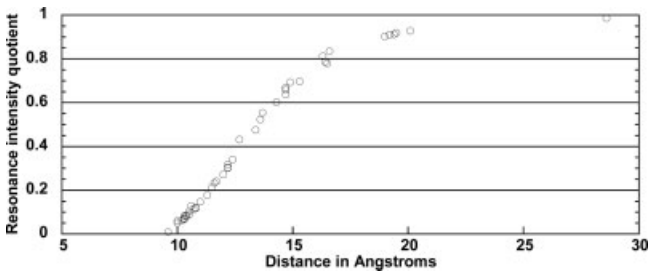

Fig. 2. Plot of E28C resonance intensity quotient versus distance from the MTSL label. Details for converting the resonance intensity quotient into distances are presented in the materials and methods. Any residue with a resonance intensity quotient >1 was excluded from the plot.

Small resonance intensity quotients are expected for residues that are adjacent to C28. This effect might extend for 5–10 residues on either side of the MTSL label, depending on the preference of the local sequence for different secondary structures.[13,14] Dynamic long-range distances are identified by small resonance intensity quotients for residues outside of this range. Figure 1 shows small resonance intensity quotients for E28C residues from L14 to T55, suggesting the presence of a compact dynamic structure.

Distance Calculations Indicate Compact Dynamic Structure

The details for distance calculations using the PRE data are described in the materials and methods section. Figure 2 shows a plot of the resonance intensity quotients for E28C versus the calculated distances. Based on the data presented in Figure 2, resonance intensity quotients that are less than 0.6 correspond to ensemble average distances of 10–15 Å.

Functionally significant sites that have ensemble average distances separated by 10–15 Å include the region essential for transactivation and MDM2 binding, (Q16-L26), the RPA70 binding domain (A39-G59), and a proline directed phosphorylation site that regulates p53 function following DNA damage (V31-M40). This result suggests that p53TAD coordinates different functions through the spatial organization of different binding sites. This is identical to the way compact globular proteins coordinate different functions with the exception that p53TAD and other IUPs have a dynamic structure when they are not bound to other proteins or DNA. This has important consequences for the function of p53TAD. In particular, the proximity of the MDM2 and RPA70 binding sites suggests that steric hindrance may play a role in binding. If this is the case, then p53TAD must 'unfold' to accommodate the binding of either protein since both MDM2 and the p53TAD binding domain of RPA70 are too large to fit in the space separating the two binding sites.[16–18]

The $1/\langle r^6 \rangle$ dependence of PRE means the measurement is biased toward detecting closer distances versus longer ones.[13,14] In the context of structure calculations for IUPs, this problem is being addressed by performing simulated annealing on an ensemble average structure instead of a single structure.[12,19] Using ensemble averaging results in a family of structures that have a distribution of gyration radii (R_g) that is skewed in the direction of larger values. What is unclear from these studies is how reliably this skewed distribution represents the equilibrium distribution. It is assumed there will be extended structures in the equilibrium distribution and their functional significance is currently being debated. In particular, recent observations show that the release of long-range interactions promotes the aggregation of intrinsically unstructured α-synuclein.[20] Our results also suggest that p53TAD may need to assume a more extended structure in order to bind either MDM2 or RPA70.

Intermolecular PRE Between RPA70 and p53TAD

To test for the presence of intermolecular PRE between p53TAD and RPA70, we used a fragment of RPA70 containing residues 1–168 ($RPA70_{1-168}$). Residues 1–128 of this fragment form a protein interaction and weak single

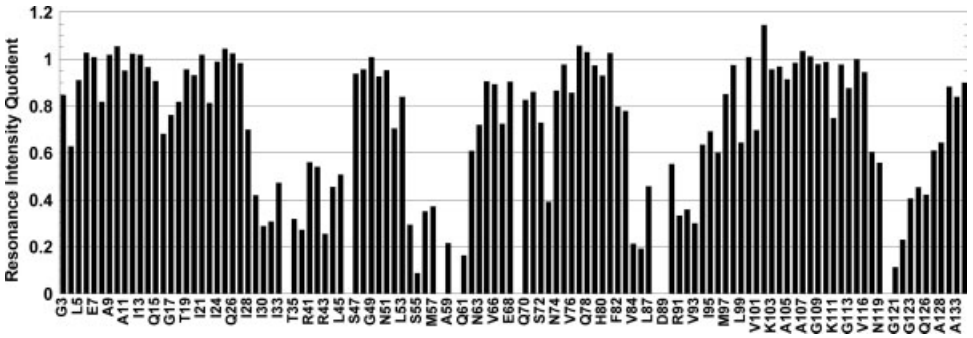

Fig. 3. Intermolecular PRE between D61C and DBD F. The vertical axis shows the DBD F resonance intensity quotient and the horizontal axis shows the DBD F residues. Resonance intensity measurements were made on a ^{15}N-labeled sample of RPA70$_{1-168}$ in complex with a molar equivalent of MTSL labeled D61C. The MTSL label was reduced by adding a fivefold molar excess of ascorbic acid and the resonance intensity measurements were repeated. The extent of MTSL labeling for D61C was verified to be >95% using mass spectrometry.

stranded DNA binding domain referred to as DNA binding domain F (DBD F). DBD F is the interaction site for p53TAD.[9] Residues 129-168 form an intrinsically unstructured linker domain.

A sample of a D61C variant of p53TAD that was MTSL labeled but not ^{15}N-labeled was added to a ^{15}N-labeled sample of RPA70$_{1-168}$. The ^{15}N HSQC resonance intensity quotient for the amide protons from the N-terminal 134 residues of RPA70$_{1-168}$ is shown in Figure 3. In Figure 3, the DBD F resonance intensity quotient is plotted as a function of RPA70 residue number. To generate the control spectrum, the MTSL spin label on D61C was reduced with a fivefold molar excess of ascorbic acid. The resulting ^{15}N HSQC spectrum of RPA70$_{1-168}$ was identical to the spectrum observed after the addition of the same amount of wild type p53TAD, demonstrating that the D61C mutant has wild type binding activity. In addition, PRE was measured for a ^{15}N-lableled sample of D61C in the absence of RPA70$_{1-168}$. This analysis was consistent with the data presented in Figure 1 and provides additional evidence for a compact dynamic structure (data not shown).

According to Figure 3, the DBD F residues with resonance intensity quotients $\leq$0.4 include I30, T35, G36, R43, L45, S54, S55, F56, A59, Q61, V84, R91, R92, V93, G121, and L122. With the exception R43, Q61, V84, G121, and L122, all of these residues have large chemical shift changes in the presence of wild type p53TAD and cluster around a basic cleft on the surface of DBD F.[9] The data presented in Figure 3 represents the first application of PRE to the problem of detecting intermolecular distances between IUPs and their binding partners.

CONCLUSIONS

Several papers have described p53TAD as an IUP.[9,21,22] These previous studies used NMR chemical shifts and coupling constants to identify transient secondary structure elements. In particular, Han and coworkers saw evidence for transient helical structure in the MDM2 binding domain of p53TAD.[22] They also saw evidence for two nascent turns in the RPA70 binding domain. More recent studies from my group confirmed the presence of these transient secondary structures.[9] Han and coworkers have also shown the two nascent turns form two additional MDM2 binding sites that overlap with the RPA70 binding site.[23] This result is interesting in light of the structural proximity between the MDM2 and RPA70 binding sites that we observe and supports our claim that p53TAD coordinates different functions through the spatial organization of different binding sites.

In this report, PRE was used to identify a compact dynamic structure for p53TAD. This result differs significantly from the previous structural studies of p53TAD. As mentioned above, previous structural studies focused on identifying elements of transient secondary structure. We have provided data suggesting that there is some global organization to the transient secondary structures and propose that this global organization is important for the function of p53TAD.

We are currently investigating the physical basis for the compact dynamic structure and preliminary data suggests it is maintained by long range interactions between the side chains of hydrophobic amino acids. The compact dynamic structure of p53TAD may also be influenced by the presence of 13 prolines. P53TAD has two PXP motifs, one PXXP motif, one PP, and five single prolines. It is reasonable to expect there are some guiding structural principles for IUPs like p53TAD that will promote our understanding of their function. To identify these principles it will be necessary to characterize the structure and dynamics of different families of IUPs using PRE and other biophysical methods.

ACKNOWLEDGMENTS

The contents of the publication are solely the responsibility of the authors and do not necessarily represent the official views of ACS or NIH. The NMR data presented in this publication was collected at the University of

Idaho Structural Biology Core Facility. This facility is funded by NIH grant number P20 RR 16448 from the COBRE program and P20 RR 16454-02 from the INBRE program. Both programs are part of the National Center for Research Resources. We gratefully acknowledge Dr. Lee Fortunato for the gift of the p53 cDNA.

REFERENCES

1. Dunker AK, Brown CJ, Lawson JD, Iakoucheva LM, Obradovic Z. Intrinsic disorder and protein function. Biochemistry 2002;41: 6573–6582.
2. Dyson HJ, Wright PE. Coupling of folding and binding for unstructured proteins. Curr Opin Struct Biol 2002;12:54–60.
3. Wright PE, Dyson HJ. Intrinsically unstructured proteins: reassessing the protein structure-function paradigm. J Mol Biol 1999;293:321–331.
4. Uversky VN. Natively unfolded proteins: a point where biology waits for physics. Protein Sci 2002;11:739–756.
5. Uversky VN. What does it mean to be natively unfolded? Eur J Biochem 2002;269:2–12.
6. Tompa P. Intrinsically unstructured proteins. Trends Biochem Sci 2002;27:527–533.
7. Iakoucheva LM, Brown CJ, Lawson JD, Obradovic Z, Dunker AK. Intrinsic disorder in cell-signaling and cancer-associated proteins. J Mol Biol 2002;323:573–584.
8. Ferreira ME, Hermann S, Prochasson P, Workman JL, Berndt KD, Wright AP. Mechanism of transcription factor recruitment by acidic activators. J Biol Chem 2005;280:21779–21784.
9. Vise PD, Baral B, Latos AJ, Daughdrill GW. NMR chemical shift and relaxation measurements provide evidence for the coupled folding and binding of the p53 transactivation domain. Nucleic Acids Res 2005;33:2061–2077.
10. Uesugi M, Nyanguile O, Lu H, Levine AJ, Verdine GL. Induced alpha helix in the VP16 activation domain upon binding to a human TAF. Science 1997;277:1310–1313.
11. Liu WL, Midgley C, Stephen C, Saville M, Lane DP. Biological significance of a small highly conserved region in the N terminus of the p53 tumour suppressor protein. J Mol Biol 2001;313: 711–731.
12. Dedmon MM, Lindorff-Larsen K, Christodoulou J, Vendruscolo M, Dobson CM. Mapping long-range interactions in α-synuclein using spin-label NMR and ensemble molecular dynamics simulations. J Am Chem Soc 2005;127:476–477.
13. Gillespie JR, Shortle D. Characterization of long-range structure in the denatured state of staphylococcal nuclease. II. Distance restraints from paramagnetic relaxation and calculation of an ensemble of structures J Mol Biol 1997;268:170–184.
14. Gillespie JR, Shortle D. Characterization of long-range structure in the denatured state of staphylococcal nuclease. I. Paramagnetic relaxation enhancement by nitroxide spin labels J Mol Biol 1997;268:158–169.
15. Battiste JL, Wagner G. Utilization of site-directed spin labeling and high-resolution heteronuclear nuclear magnetic resonance for global fold determination of large proteins with limited nuclear overhauser effect data. Biochemistry 2000;39:5355–5365.
16. Kussie PH, Gorina S, Marechal V, Elenbaas B, Moreau J, Levine AJ, Pavletich NP. Structure of the MDM2 oncoprotein bound to the p53 tumor suppressor transactivation domain. Science 1996; 274:948–953.
17. Bochkareva E, Kaustov L, Ayed A, Yi GS, Lu Y, Pineda-Lucena A, Liao JC, Okorokov AL, Milner J, Arrowsmith CH, Bochkarev A. Single-stranded DNA mimicry in the p53 transactivation domain interaction with replication protein A. Proc Natl Acad Sci USA 2005;102:15412–15417.
18. Jacobs DM, Lipton AS, Isern NG, Daughdrill GW, Lowry DF, Gomes X, Wold MS. Human replication protein A: global fold of the N-terminal RPA-70 domain reveals a basic cleft and flexible C-terminal linker. J Biomol NMR 1999;14:321–331.
19. Lindorff-Larsen K, Kristjansdottir S, Teilum K, Fieber W, Dobson CM, Poulsen FM, Vendruscolo M. Determination of an ensemble of structures representing the denatured state of the bovine acyl-coenzyme a binding protein. J Am Chem Soc 2004;126:3291–3299.
20. Bertoncini CW, Jung YS, Fernandez CO, Hoyer W, Griesinger C, Jovin TM, Zweckstetter M. Release of long-range tertiary interactions potentiates aggregation of natively unstructured α-synuclein. Proc Natl Acad Sci USA 2005;102:1430–1435.
21. Bell S, Klein C, Muller L, Hansen S, Buchner J. p53 contains large unstructured regions in its native state. J Mol Biol 2002; 322:917–927.
22. Lee H, Mok KH, Muhandiram R, Park KH, Suk JE, Kim DH, Chang J, Sung YC, Choi KY, Han KH. Local structural elements in the mostly unstructured transcriptional activation domain of human p53. J Biol Chem 2000;275:29426–29432.
23. Chi S-W, Lee S-H, Kim D-H, Ahn M-J, Kim J-S, Woo J-Y, Torizawa T, Kainosho M, Han K-H. Structural details on MDM2-P53 interaction. J Biol Chem 2005;280:38795–38802.